琉球大学学術リポジトリ

FE simulation of stress field and crustal deformation around Southern Ryukyu Arc

メタデータ	言語:
	出版者: 琉球大学理学部
	公開日: 2009-04-06
	キーワード (Ja):
	キーワード (En):
	作成者: Suzuki, Ryota, Hayashi, Daigoro, 林, 大五郎
	メールアドレス:
	所属:
URL	http://hdl.handle.net/20.500.12000/9530

47

FE simulation of stress field and crustal deformation around Southern Ryukyu Arc

Ryota Suzuki and Daigoro Hayashi

Simulation Tectonics Laboratory, Faculty of Science
University of the Ryukyus, Okinawa, 903-0213, Japan

Abstract

Finite element (FE) modeling has designed to investigate dynamics of Southern Ryukyu Arc based on synthesized stress-strain, velocity, geology and seismicity data. Result of horizontal minimum stress (σ Hmin) orientation is compared to present stress distribution. We constructed 1300 km×600 km model for Southern Ryukyu Arc. FE model was bounded along the Ryukyu Trench. Studied region is divided into 3 domains: arc region, Okinawa Trough and continental margin. As displacement velocity is 9.0 cm/yr in Taiwan, we set up NW boundary displacement of 2000 m that correspond to c.a. 20,000 year on Ryukyu Trench to Taiwan. Four boundary conditions under 1, 10 and 30 km depth are considered. In addition, single domain model is also constructed. Total 16 experiments are performed. Result of σ Hmin orientation shows good agreement with T-axis distribution in Taiwan and Ryukyu Arc (Kubo and Fukuyama, 2003; Otsubo and Hayashi, 2003). In addition, large stress concentrates on eastern area of Taiwan while in Okinawa trough, computed σ Hmin orientation is arc-parallel which is inconsistent with observed σ Hmin orientation. Depth affects greatly to the stress magnitude but not to stress orientations in the Ryukyu Arc. It is found that orientation of σ Hmin is principally controlled by rock domain properties of major structural zones and the direction of convergence of the Philippine Sea plate relative to Eurasia. Direction of displacement vector is good agreement with that of observed velocity field in Taiwan, while direction of displacement vector is trending NW or W in Okinawa trough and Ryukyu Arc, indicating that this model does not fit in this point.

1. Introduction

The Ryukyu Arc-Trench system located continental margin of Eurasia and which has evolved next to Taiwan orogen (Fig. 1). Geological survey has started from more than hundred years ago and summarized by Kizaki (1985 and references therein). In Arc region, geologic observation has contributed to the tectonic history in term of structural geology (Fujii and Kizaki, 1983) and paleostress analysis (Kuramoto and Konishi, 1989; Fabbri and Fournier, 1999; Fabbri, 2000; Fournier et al., 2001; Otsubo and Hayashi, 2003; Teramae and Hayashi, 2004). The present crustal deformation of this area is described fully in term of Global Positioning System (GPS) studies (Imanishi et al., 1996; Nakamura, 2004; Nishimura et al., 2004; Watabe and Tabei, 2004) as well as focal mechanism moment tensor analysis (Shiono et al., 1980; Fournier et al., 2001; Kubo and Fukuyama, 2003). GPS observation shows southward motion of the southern Ryukyu Islands. According to the moment tensor analysis, present kinematics of the Ryukyu Arc is characterized by arc parallel extension. On the other hand, Okinawa trough, which is the back-arc basin of the Ryukyu Arc, is in active rifting stage. Recent marine geological studies have contributed to the tectonic history, spreading mode and spreading rate of Okinawa Trough (Letouzey and Kimura, 1986; Furukawa, 1991; Sibuet et al., 1995; Park et al., 1998). Present kinematics of Okinawa trough is represented by both arc-parallel and arc-perpendicular extension. That is also supported by precise GPS observation (Nishimura et al., 2004).
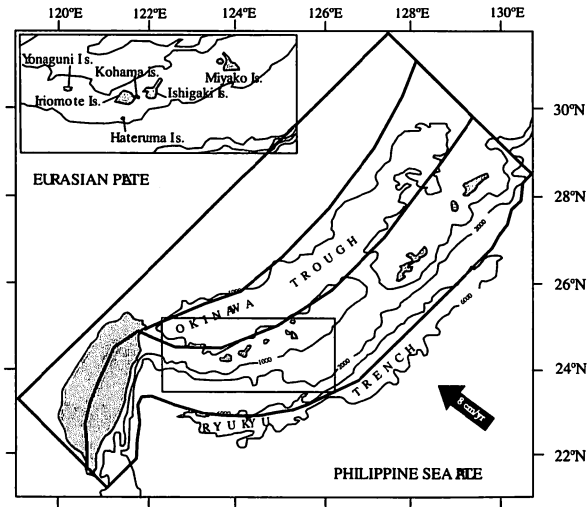
Fig.1. Tectonic setting of the Ryukyu Arc-Trench system and associated back arc basin, Okinawa trough. The solid arrow
represents the direction of plate convergence after Seno et al. (1993). The model is superposed.
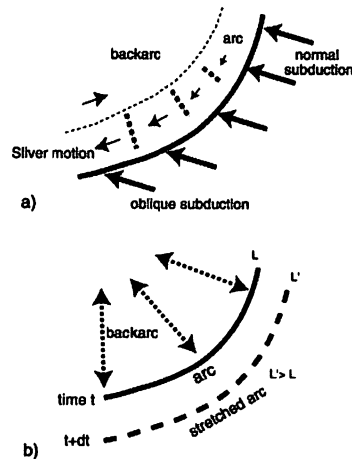

Fig. 2. Two possible explanations for mechanism of arc parallel extension (Kubo and Fukuyama, 2003).

General link between arc parallel extension in the arc and arc perpendicular extension in the back-arc have
been explained by trench retreat model (Viallon et al., 1986; Hu et al., 1996). However, it is reported that the
existence of Quaternary E-W strike slip shear zone in Yonaguni Island near Taiwan-Ryukyu junction zone to
the east 123.5°E (Kuramoto and Konishi, 1989; Otsubo and Hayashi, 2003). Therefore, it indicates that effect
of oblique subduction of Philippine Sea (PHS) plate. PHS plate is obliquely, not normally subducting at the
Southern Ryukyu Arc. Convergence rate of PHS plate and Eurasian (EUR) plate is 5-9 cm/yr for NW
estimated by Seno et al. (1993). There could be two possible factors controlling the arc parallel extension (Fig.
2): (a) forearc sliver by oblique subduction of PHS plate or (b) entire Ryukyu Arc goes southward and
stretches itself (Kubo and Fukuyama, 2003). Then, in this study we examine to use FE method to attempt to
explain the relationship between stress distribution and convergent kinematics in and around the Southern

Ryukyu Arc. FE method is powerful technique to calculate the stress, strain and displacement.

Numerous FE modeling studies have been carried out about the Ryukyu Arc in plan view (Viallon et al., 1986; Hayashi and Iguchi, 2000; Otsubo and Hayashi 2003; Nakamura 2006), and in section view (Lu and Hayashi 2002; Watabe and Tabei 2006) and similarly several FE modeling also applied in Taiwan (Hu, et al., 1996, 2001). Hu, et al. (1996) constructed plane stress elastic and elastic-plastic FE model of Taiwan and surrounding area taking into account present day stress distribution and plate motion. According to them, most of stress field of Taiwan is explained by extrusion of PHS plate to EUR plate but extensional field in Okinawa trough back-arc spreading and its extend of Ilan Plain was not simulated. Therefore, Hu et al. (1996) use another model including southward displacement on the Ryukyu Trench. Using FE model, Lu and Hayashi (2001) analyze section profile that perpendicular to the Ryukyu Arc system with various boundary conditions to simulate rifting in Okinawa trough. Otsubo and Hayashi (2003) studied neotectonic stress field by FE modeling in the Southern Ryukyu Arc without rock failure. Nakamura (2006) also has simulated velocity field of this region by means of FE modeling based on observed data without adding trench retreat force on the Ryukyu Trench. His study suggests that the possibility of rotation force in Taiwan have significance roll in the Southern Ryukyu Arc.

The main aim of this study is to construct synthetic stress field model in the Southern Ryukyu Arc using FE simulation. To construct reasonable model, we have tested under variable boundary conditions, physical property of rocks and depths.

2. Tectonic setting of the Southern Ryukyu Arc

The Ryukyu Arc-Okinawa Trough system is one of the several arc and back-arc systems along the margin of the East Asia and is convergent boundary between the PHS plate and EUR plate (Fig. 1). Along the Ryukyu Trench, PHS plate is subducting under EUR plate. Ryukyu Arc is divided morphologically as well as geologically into three groups: north Ryukyu (Osumi Islands), central Ryukyu (Amami-Oshima and Okinawa Islands), and south Ryukyu (Miyako and Yaeyama Islands) (Kizaki 1986). These islands are separated by the Tokara Channel and the Kerama depression. Both of which are identified by the left?lateral strike-slip faults. The pre-Miocene sediments of the north and central Ryukyu Are regarded as the extension of those of the southwest Japanese Islands, whereas the pre-Miocene geology of the south Ryukyu is similar to that of Taiwan. Yaeyama metamorphic rock is thought to be the basement rock of the south Ryukyu because this is the oldest rock (Kizaki 1986).

The stratigraphy of the Southern Ryukyu Arc is given in Fig. 3. In the following, we introduce geological setting of the Southern Ryukyu Islands. The description of following sections 2.1 to 2.6 was originally translated by D. Hayashi from the article written in Japanese by Kizaki (1985) to construct a part of the paper by Otsubo and Hayashi (2003).

2.1. Miyako Island

The Miyako Island is the northernmost island of the Southern Ryukyu Arc, and lies about 250 km southwest from Naha in Okinawa Island and about 100 km northeast from the Ishigaki Island (Fig.1). Miyako Island shows a flat triangle with two equal sides. The length of NW-SE side is about 30 km. The Shimajiri Group is the basement of the island, which consists of Miocene to lower Pleistocene formation, and is unconformably covered by the Ryukyu Group. Several faults run along NW-SE and NNW-SSE in the island.

Southwestern coast shows a steep scarp composed of the Ryukyu Group with a few meters to about 40 m in height. Base of the Shimajiri Group is exposed along the scarps of the eastern side of the island. It is difficult to observe the outcrop of the group in the southern side because of its steep scarps. The Shimajiri Group consists of mudstone and sandy mudstone, and shows soft to semi-consolidated state in one of the weathered outcrops. Outcrops show generally weathering in its upper part. Thick formation at several outcrops contains clay. In the alternation of sandy mudstone and mudstone, some sandy mudstone beds protruded by differential erosion. The Shimajiri Group shows the anticline whose fold axis directs to NE-SW and plunges to SW having is 4 to 6 km wavelength. The Ryukyu Group (Ryukyu Limestone) covers extensively the island and its lithostratigraphic column is observed in the steep scarps of the southern coasts. The group consists of basal conglomerate, coral limestone, rudstone and floatstone from lower to upper, which shows transgressive facies from coarse (deep) to fine (shallow). This group shows anticline whose fold axis directs to NW-SE and which passes through the center of the island. Both limbs of the anticline dip about 10 degrees. There are many faults whose offset is less than 30 m and whose strike is parallel to fold axes, and they show stair step shape. The anticline forms a low ridge hill of the island. The undulation of surface reflects undulation of the basement of the island. Cuesta is characteristic to the Miyako Island and is derived from the fault topography (Kizaki, 1985; Otsubo and Hayashi, 2003).

2.2. Ishigaki Island

The Ishigaki Island is an easternmost island of the Yaeyama Islands, which lies about 350 km west-southwest from Naha in Okinawa Island and about 200 km east from northeastern edge of Taiwan (Fig. l). Yaeyama metamorphic rocks are the basement of the island, which are divided into the Tomuru Formation and the Fusaki Formation in terms of their metamorphic phase and degree, and structure. The Yaeyama metamorphic rocks are unconformably covered with the Miyaragawa Formation (platform-type limestone), the Nosoko Formation (pyroclastic rocks and green tuffs) and the Quaternary gravels and limestones. The Miocene intrusive granite, the Omoto Granite, is also existed in the island. There are no clear major faults in the island. The oldest rocks of the island may be represented by the Tomuru Formation of the Yaeyama metamorphic rocks of the Southern Ryukyu Arc, which are composed of greenschist, blueschist, silious schist, pelitic schist, metagabbro of the glaucophane schist facies and also pillow lavas and hyaloclastic rocks in less metamorphosed areas. The metamorphic Tomuru Formation is shown to be distributed only throughout the Yaeyama Islands but also in the area of the Miyako Islands because the glaucophane schist-bearing conglomerate occurs in the basal part of the Shimajiri Group of Pliocene age in the islands. The radiometric ages of the metamorphism have been dated as Jurassic: 159-175 Ma by the K-Ar method and 195 Ma by the Rb-Sr method. According to the frequency diagram of the radiometric ages of the high-pressure metamorphic rocks from southwest Japan and Taiwan, the age of the Yaeyama metamorphic rocks is to be correlated with the older episode of the Nagasaki metamorphic rocks and with the younger episode of the Sangun metamorphic rocks in the Inner Belt of southwest Japan. It is therefore suggested that the Yaeyama metamorphic rocks could be attributed to the high-pressure metamorphic rocks of the Inner Belt of southwest Japan and also the original rocks could be Triassic to Paleozoic, similar to other high-pressure metamorphic rocks in southwest Japan and Taiwan. Structural analysis has revealed two main deformation phases; first phase folding, with a NW-SE axis, is principal and associated with a high pressure metamorphism having preferred mineral lineation parallel to the fold axis, and the second phase, of close to open minor folds with E-W axis, superimposes on the first phase folding to result in dome and basin structures in some places (Fujii and Kizaki, 1983).

The Fusaki Formation of the Yaeyama metamorphic rocks, composed of phyllite, sandstone, chert and conglomerate without greenstone, has been regarded as a lower grade chlorite-sericite phyllite of the metamorphics of the same age. However, the formation, together with the Eocene Nosoko Formation, is over thrust by the Tomuru Formation and it is not deformed by the NW-SE trending folds of the first phase but only by the E-W trending, open and gentle folds of the second phase. A chert bed of the formation produces radioralia older than lower Cretaceous. So, the Fusaki Formation may have been deposited between the Jurassic and lower Cretaceous, after the metamorphism of the Tomuru Formation. The Fusaki Formation is distributed in the southern part of Ishigaki Island and to the north of Miyako Island where 38 Ma phyllite (K-Ar method) has been obtained from a bores core. However, such an Eocene metamorphism is not known in the North-Central Ryukyu and further north, so that the rock probably belongs to the Fusaki Formation.

The Miyaragawa and Nosoko Formations of Eocene age occur only in the Yaeyama Islands of the Southern Ryukyu, in addition to the Eocene formation of the Shimanto Supergroup of the North-Central Ryukyu. The Miyaragawa Formation, composed of limestones and sandstones, contains various foraminifera such as *Nummulites, Discocyclina, Pellatispira.* Some of these fossils are also found in the tuffs and tuffaceous sandstones of the Nosoko Formation, which is composed of pyroclastic rocks and andesite lavas. The Miyaragawa Formation represents a littoral facies whereas the Eocene flysch sediments occur in the Shimanto Supergroup, and further deformation and meta- morphism are not recognized in the Miyaragawa and Nosoko Formations but do clearly in the supergroup of North-Central Ryukyu. The paleomagnetic investigation of the Nosoko Formation revealed that a clockwise rotation of $40°$ took place after the deposition of the formation, probably in the Oligocene. The Eocene volcanism was only developed in the southern Ryukyu whereas the Miocene "Green Tuff Volcanics" are distributed throughout the north-central Ryukyu from Kyushu; nevertheless the rock facies are quite similar to each other. However, the pyroxene andesites of the southern Ryukyu indicate a lower alkali-lime index (58.3) than the Miocene andesites (61.8) of the north-central Ryukyu. The Ryukyu Group exposed in the Ishigaki Group is called the Ohama Formation. The formation is mainly divided into the Ryukyu Limestone and Sand and Gravel bed (Kizaki, 1985; Otsubo and Hayashi, 2003).

2.3. Kohama Island

The Kohama Island is a small island, which lies about 15 km west from the Ishigaki Island and about 3 km east from the Iriomote Island (Fig. 1). However, the Kohama Island is the important island to study stratigraphic relationship of strata in Yaeyama area because all of the strata distributed in the Yaeyama Islands are existed in the island. The Hunazaki metamorphic rock is the basement of the island, which is compared with the Tomuru Formation, and is unconformably covered by the Koki Limestone, the Komasaki Formation (pyroclastic rock), the Birumazaki Formation (alternate bed of sandstone and mudstone) and Quaternary Gravels and Limestones. No clear major fault is existed in the island. The Koki Limestone, the Komasaki Formation and the Birumazaki Formation are correspond to the Miyaragawa Formation, the Nosoko Formation of the Yaeyama Group, respectively. Quaternary Gravels and Limestones are composed of terrace conglomerate and Ururo limestone (Kizaki, 1985; Otsubo and Hayashi, 2003).

2.4. Iriomote Island

Iriomote Island is the fifth large island, which lies about 20 km west from the Ishigaki Island and about 180

km east from northeastern edge in Taiwan (Pig. 1). In Iriomote Island, metamorphic rock of the Tomuru Formation is the basement and is unconformably covered by the Miyaragawa Formation, the Nosoko Formation and the Iriomote Formation (Yaeyama Group), the Sonai Conglomerate and the Sumiyoshi Formation (Ryukyu Group) (Quaternary gravel and limestone). The Iriomote Formation is widely exposed in the Iriomote Island. No clear major fault (lineament) is existed in the island.

The Tomuru Formation in the island consists of basic schist, muddy schist, quartzitic schist and metamorphic gabbro. The bed trends northeast to north and dips northwestward. The Miyagawa Formation is the platform type limestone, which is exposed in a limited area at the upper reaches in Yonara river. The formation lies horizontally whose thickness is about 20 m. The Nosoko Formation is divided into two parts. Lower part of the formation mainly consists of andesitic volcanic breccia, andesitic tuff breccia and andesitic lava, while the upper part consists of dacitic lava, rhyolitic tuff, rhyolitic breccia tuff and rhyolitic lava. Dacitic dyke is also exposed in the formation. The thickness of the formation is about 300 m. Pre-Miocene formations, the Tomuru, the Miyaragawa and Nosoko Formations are exposed in a limited area in the northeastern part of region. The Iriomote Formation is composed of conglomerate, sandstone and siltstone, coal bed, and calcareous sandstone, which covers unconformably the Nosoko Formation. The thickness of this formation is about 700 m. The bed trends northeast and dips westward. The formation is lithologically divided into A, B, C, D, E, F and G beds. In particular, the bed F is called Utibanare coal-bearing member. The Sonai Conglomerate is composed of sandstone, calcareous sandstone and shell limestone whose gravels are pebbles or flat gravel in 6 cm diameter. All the Sonai Conglomerates is derived from the Iriomote Formation. However, the age of the formation remains unknown. Conglomerate, sandstone and limestone included in the Ryukyu Group are called the Sumiyoshi Formation. The bed is found in a scattered pattern along the coast in the island. The bed is considered the upper part of the Ryukyu Group (Kizaki, 1985; Otsubo and Hayashi, 2003).

2.5. Hateruma Island

The Hateruma Island is a small island and the southernmost island of the Ryukyu Islands, which lies about 20 km south from the Iriomote Island (Fig. 1). Although geological character in the island looks like that of the Kikai Island, southern part in the Okinawa Island and the Miyako Island, pre-Quaternary basement rock (Shimajiri Group) shown in other islands (e.g. Miyako Island) have not been exposed in the island. Therefore, most of the formations in the island are belong to the Ryukyu Group. Several major faults run along NW-SE and WNW-ESE in the island, which may be strike-slip faults. Basement of the island is dark bluish gray mudstone observed in a limited area. The formation is correlated with the Shimajiri Group by the lithofacies, color, degree of consolidation and the relationship to the Ryukyu Group. The Ryukyu Group is mainly composed of limestone and exposured widely in the island. The group has formed three steps terrace, and divided into three formations the Huka Formation, the Hateruma Formation and the Takanazaki Formation. Yamada and Matsuda have divided this group into four units. The unit 1 is only accumulative or backed develop type and unit 2, 3 and 4 are advance develop type (Kizaki, 1985; Otsubo and Hayashi, 2003).

2.6. Yonaguni Island

The Yonaguni Island is the hexagonal-shape island and the westernmost island of the Ryukyu Islands, which lies about 170 km east from the northeastern edge of Taiwan (Fig. 1). The Yaeyama Group, which is composed of alternate bed of sandstone and mudstone is the basement of the island and is unconformably

covered by mainly the Ryukyu Group (limestone) and the Quaternary deposits. Several faults run along NW-SE, NE-SW and E-W in the island. Shape of the island is defined by sevenal faults. Kizaki (1985) reported that three fault systems (NW-SE, NE-SW and E-W) are composed of steeply normal faults. In the Yaeyama Group, the cycle of alternation of the group varies in degree. Most of the Yaeyama Sandstones are feldspathic wackes, white bivalves, including oyster, and terrestrial plants are common in the Yaeyama Group throughout the island. Some sedimentary structures such as channel and turbidite sequences are observed. Paleocurrent directions are approximately from north to south (Kuramoto and Konishi, 1989). The thickness of the formation is approximately estimated to be over 1000 m. The formation shows that same unit is observed several times because the bed is cut by normal fault. The bed strikes to northwest and dips southeastward. The Ryukyu Group, which overlaps unconformably the Yaeyama Group is divided into the lower Donan Formation and the upper Ryukyu Limestone. The Donan Formation is divided into two fades; sand and pebble and boulder. The former is mainly composed of very fine to fine sand and flat pebbles of feldspathic wacke which is derived from the Yaeyama Group. The thickness of the formation is less than 20 m. Two facies are recognized in the upper Ryukyu Limestone; detrital and coralliferous. The thickness of the formation attains 40 m in maximum, and it varies markedly with the local variation of the basement relief. The lowest terrace formed of the coralliferous facies lies at 5-6 m above the present mean tide level along the northern coast. The terrace is dated to be the Last Interglacial (about 0.125 Ma), by 230Th coral age.

Quaternary deposits are divided into the Urabu sand and gravel and the raised reef limestone. In particular, sedimentation of the Urabu sand and gravel relates to the fault formation and tilting movement of the island because the bed is exposed along the major fault system and the thickness increases from north to south within the basin (Kizaki, 1985; Otsubo and Hayashi, 2003).

2.7 Complex structure in the TRFZ (Taiwan-Ryukyu fault zone)

The Yaeyama Ridge, which is a 40-60 km wide and E-W trending accretionary wedge, forms the toe of the Ryukyu margin offshore east Taiwan and the southernmost Ryukyu arc-forearc zone. The Gagua Ridge is subducting obliquely beneath the Yaeyama Ridge on the Ryukyu Trench along $123°E$ (Hsu et al., 1996; Schnurle et al., 1998; Lallemand et al., 1999). The Gagua Ridge is the oceanic ridge about 2 km high and 25 km wide. From multi-channel deep seismic reflection profile study, Schnurle et al. (1998) concluded that the oblique subduction of the Gagua Ridge has not only affected the accretionary wedge structure but also the arc basement of the south Ryukyu margin. Numerous marine studies have been carried out (e.g. geologic, geomorphologic, seismologic and gravity). Although seismo-tectonics and subduction history of junction zone are complex, it is important to clear the mechanism of strain partitioning on PHS-EUR subduction zones.

2.8 Taiwan collision zone

The island of Taiwan is located along a part of the convergent boundary between the PHS plate and EUR plate, where collision as well as subduction processes occur. The PHS plate is subducting beneath the EUR plate at the Ryukyu Trench and overriding the crust of the South China Sea at the Manila Trench. The SE-facing Ryukyu Arc-and-Trench system extends from the southern Kyushu (Japan) to the east of Taiwan. The Ryukyu Subduction Zone is associated with the back-arc spreading of the Okinawa Trough, which ends to the west in the Ilan Plain of northeastern Taiwan, where extensional seismic activity occurs (Tsai, 1986). In contrast, the W-facing Luzon-Manila Arc and-trench system extends from Philippines to about $22°N$, where it

Fig.3 Suzuki and Hayashi

	Ma	Yonaguni	Hateruma	Iriomote, Kohama	Ishigaki	Miyako
Holocene	0.01	Urabu sand and Gravel				
Pleistocene	2	Ryukyu G.	Ryukyu G.	Ryukyu G.	Ryukyu G.	Ryukyu G.
Pliocene	5		Shimajiri G.			Shimajiri G.
Miocene	10 / 15 / 20	Yaeyama G.		Yaeyama G.	Omoto Granite	
Eocene	40 / 45 / 50			Nosoko F. / Miyaragawa F.	Nosoko F. / Miyaragawa F.	
Pre-Tertiary				Tomuru F.	Fusaki F. / Tomuru f.	

Fig. 3. Stratigraphy of the Southern Ryukyu Arc (after Otsubo and Hayashi, 2003).

merges into the mountain ranges of Taiwan. As Fig. 4 shows, Taiwan can be divided into two major tectonic provinces separated by the active Longitudinal Valley Fault (Ho, 1986). Tile narrow eastern province, including the Coastal Range and the two islands of Lutao and Lanhsu, is a remnant Neogene island arc usually interpreted as the leading edge of the PHS plate, that is the northern extension of the Luzon Arc. The large western province, which includes most of Taiwan, is usually divided into several stratigraphic and structural units, based on rock types and degrees of metamorphism. These units are generally bounded by major faults and thrusts. The main units are from east to west: (1) the Central Range (2) the Western Foothills and (3) the Coastal Plain (Fig. 4). The Central Range of Taiwan is characterized by the presence of Tertiary metamorphism, in contrast with the adjacent non-metamorphic fold-and thrust belt of the Western Foothills (Ho. 1986). The pre-Tertiary basement, which has been affected by Neogene greenschist facies as well as by higher grades of polyphase Mesozoic-Cenozoic metamorphism, crops out in the eastern flank of the Central Range. The axial ridges and the western flank constitute the Slate Belt. In the Western Foothills, Miocene, Pliocene and Early Pleistocene shallow marine to shelf clastics sediments thicken from north to south and east to west. These sediments are affected by WNW-vergent folds and low-angle thrust faults. The Coastal Plain is composed of Quaternary alluvial deposits derived from the Central Range and the Western Foothills. It is widely considered that the western tip of Okinawa Trough is the Ilan Plain of northeastern Taiwan, based on bathymetric trends and distribution of earthquakes (Ho, 1986). According to Letouzey and Kimura (1986), the Okinawa marginal basin opened due to crustal extension behind the Ryukyu Arc in the Asian continent since about 2 Ma ago. The fold-and-thrust belt of Taiwan advanced northwestward, while the growth of orogen was propagated southwestward along the passive continental margin of the EUR plate (Suppe, 1981; 1984) (Quoted from Hu et al. (1996)).
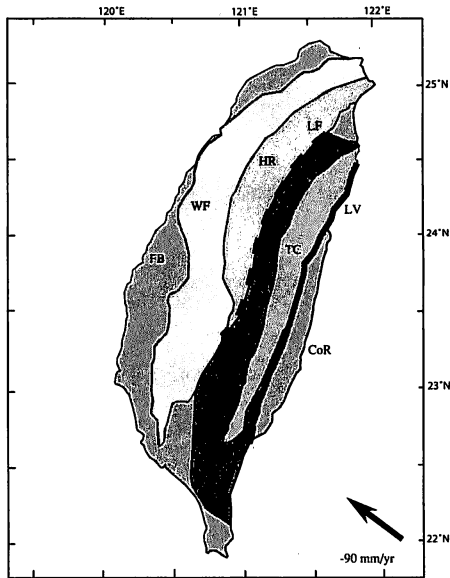
Fig. 4. Geological context of Taiwan (after Ho, 1986). FB: the foreland basin, WF: the Western Foothills, HR: the Hsueshan
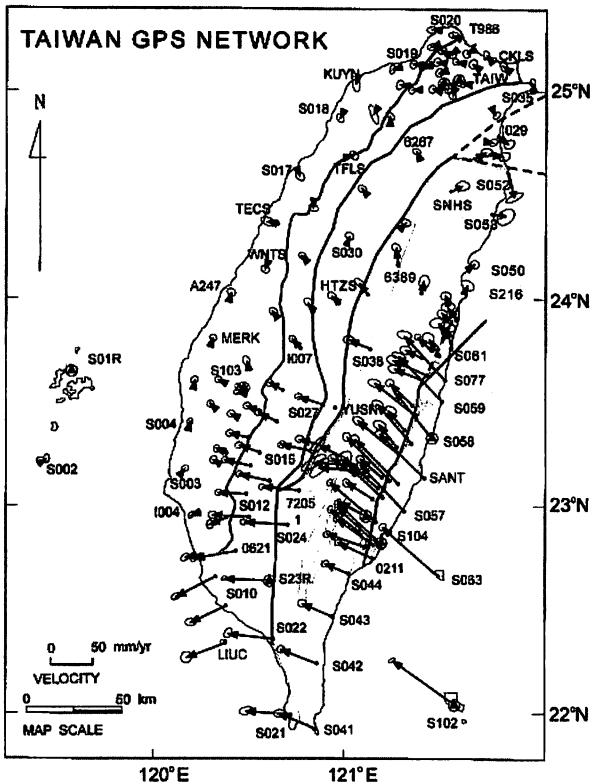Range, BS: the Backbone Slates, TC: the Tananao Complex, LV: the Longitudinal Valley.

Fig. 5. GPS derived velocity field of Taiwan relative to Paisha, Penghu (S01R) (after Hu et al. 2001).

3. Opening of the Okinawa Trough

The Okinawa Trough (OT) is a back-arc basin currently opening behind the Ryukyu Arc-Trench system (Fig. 1). According to Fournier et al. (2001), it has been the site of crustal stretching and thinning since the Miocene (Letouzey and Kimura, 1986). Rifting in the northern Okinawa Trough occurs within a series of N60°E subgrabens aligned obliquely to the N30°-N45°E structural trend of the arc and trench (Sibuet et al., 1995). Conversely, in the southern Okinawa Trough the N80°-90°E trending subgrabens strike parallel to the E-W regional trend. The crustal thickness along the trough axis decreases from 27-30 km in the northern part near Taiwan (Iwasaki et al., 1990). Such crustal thickness indicates that the Okinawa trough is still in a rifting stage. The formation of back-arc spreading system has been controversial (Tamaki and Honza, 1991). Paleomagnetic studies suggest that the OT has opened episodically since the late Miocene (Miki, 1995).

4. Present-day velocity field

In Taiwan, Hu et al. (2001) performed precise velocity field observation and found that convergence rate across the Taiwan plate boundary is estimated about 9 cm/yr (Fig. 5). This is same as the rate of GPS-derived plate model REVEL (Sella et al., 2002).

In Ryukyu Arc, Nakamura (2004) studied GPS analysis to investigate crustal deformation and found that the velocity of plate motion is 2 cm/yr in Miyako and 3 cm/yr in Ishigaki and 6 cm/yr in Yonaguni and its direction are southeast to south (Fig. 6).

The current opening of the OT is estimated by geodetic measurements (Imanishi et al., 1996). If the opening rate of the back-arc cannot be neglected in comparison to the relative plate motion, then the actual relative velocity at the plate boundary may be different from the conventional plate model. In a previous study, the instantaneous velocity field of the Ryukyu Arc was not well resolved because of trade-offs between the opening of the OT, and eastward motions of the Amurian plate (AM) and the South China block (SC). Nishimura et al. (2004) estimated the rigid block motions of GPS sites in the Ryukyu Arc relative to the AM and the SC using a three-block model. The present opening rate of the OT is estimated at 5 cm/yr in the
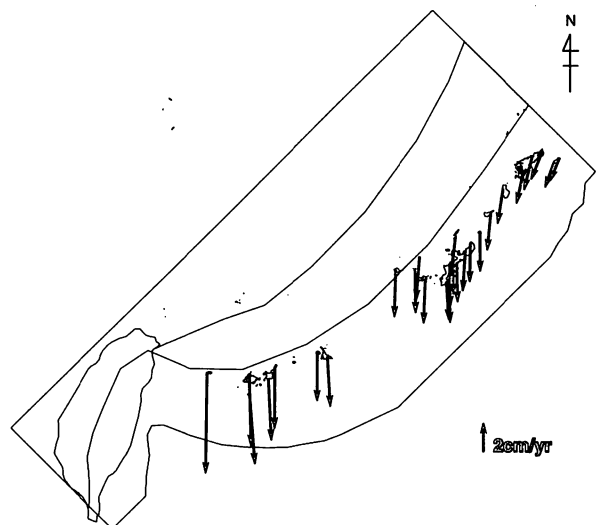

Fig. 6. Velocity field of Ryukyu Arc. All vectors are relative to Eurasian plate (Shanghai VLBI) (after Nakamura, 2004).

southwestern OT and 1 cm/yr in the northeastern OT, which is on the same order of magnitude as the relative plate velocity between the PH and the EU (Seno et al., 1993). Thus, the plate convergence may not be the only significant factor in creating the observed forearc deformation, but the entire system from the subduction zone to the back-arc should be properly taken into account, as well as the plate boundary evolution (Quoted from Kubo and Fukuyama (2003)).

5. Stress distribution in the Southern Ryukyu Arc

5.1 Focal mechanism moment tensor solutions

To investigate the detailed stress field along the Ryukyu Arc and the Okinawa Trough, focal mechanisms of small earthquakes are absolutely necessary, especially in the Ryukyu Arc. However, because of the limited station distribution in the islands, it is difficult to determine focal-mechanism solutions. Fournier et al. (2001) used 22 year worth of Harvard Centroid Moment Tensor solutions (HCMT) in addition to geological and topographical data to investigate the stress field in the Ryukyu Arc and the OT. Their dataset covered a wide region in the OT, but included only two focal mechanisms in the Ryukyu Arc (forearc). Apparently, the number of focal mechanisms was not sufficient in the forearc to discuss the present status of the mechanical interaction among the subducting plate, forearc, and back-arc.

Kubo and Fukuyama (2003) investigated the stress field along the Ryukyu Arc and the Okinawa Trough using regional NIED MT (National Research Institute for Earth Science and Disaster Prevention moment tensor solutions) and global HCMT catalogs. Using the combined dataset of 4 years of data from the NIED MT catalog and 24 years of data from the HCMT catalog, they found an arc-parallel extensional stress province along the forearc of the Ryukyu Arc and observed a detailed extensional stress field in the Okinawa
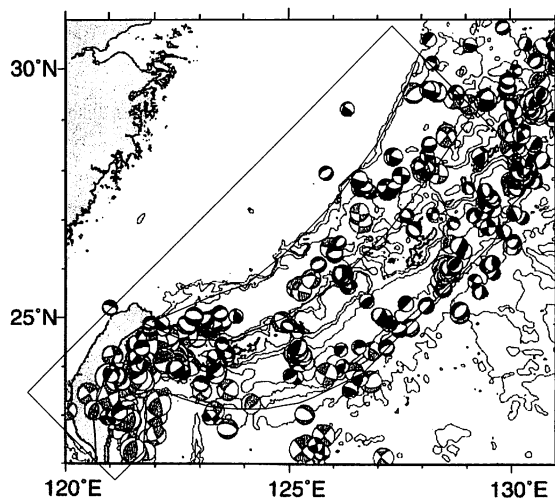

Fig. 7. Focal-mechanism solutions of shallow earthquakes (depth <30 km) determined by NIED MT catalog (Jan. 1997-Oct. 2001) and HCMT catalog (Jan. 1977-Apr. 2001) (after Kubo and Fukuyama, 2003).

Trough (Figs. 7 and 8). This arc-parallel extension is observed in the entire region of the Ryukyu Arc except at its northeastern end. This stress field is clearly separated from the back-arc extensional stress field in the Okinawa Trough by the volcanic chain. Along the Okinawa Trough, an arc-perpendicular extensional stress
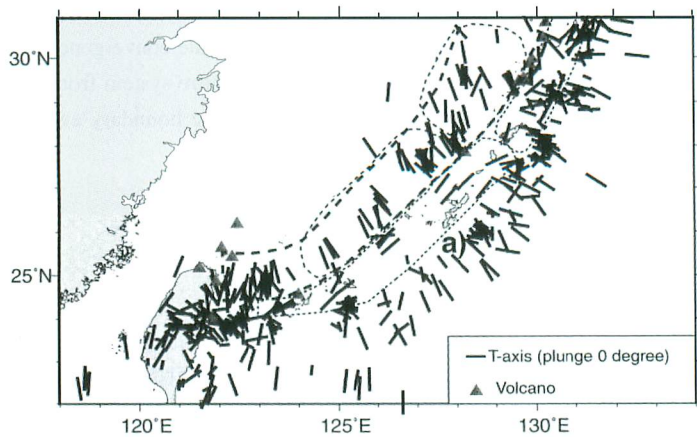
Fig. 8. T-axis distribution (modified after Kubo and Fukuyama 2003).

field is observed in the southeastern and central Ryukyu Arc, while in the northeastern Okinawa Trough, the direction of the extensional axis is oblique to both the arc normal direction and the direction of plate motion (Quoted from Kubo and Fukuyama (2003)).

Nakamura (2007) used stress inversion method to clarify stress field of subducted PHS plate in the Taiwan-Ryukyu junction zone. According to their analysis, down-dip compression and plate perpendicular extensional axis are dominant in the Ryukyu Arc side. But in Taiwan down dip extension and plate parallel compressional axis are dominant. PHS plate is obliquely subducting with bending so that those complex stress field has occur.

5.2 Quaternary stress/ paleo-stress field

Fault?slip data of meso-scale fault are measured from which can be seen in outcrop scale. The fault-slip data are composed of strike and dip of faults, and trend and plunge of slickenlines on the fault planes. Effective numerical methods have developed to separate stresses from polyphase fault-slip data (Teramae and Hayashi, 2004). Using that new method, Otsubo and Hayashi (2003) detected that Quaternary stress on the
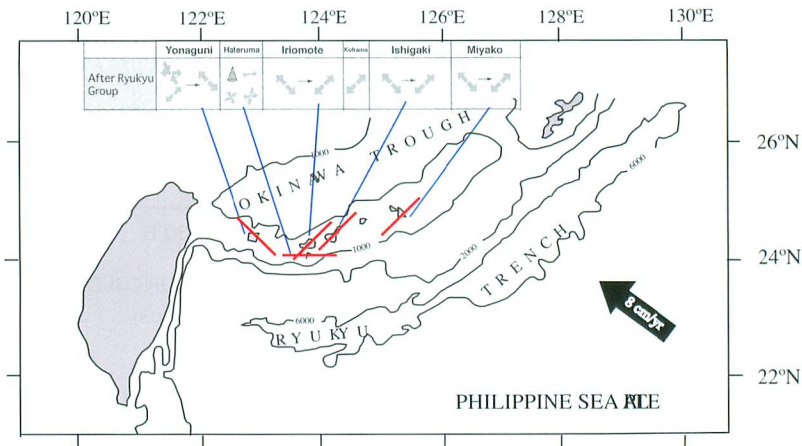

Fig. 9. Quaternary fault slip data in Southern Ryukyu Arc (after Otsubo and Hayashi, 2003).

southern Ryukyu Arc is divided into three groups: Miyako Island and Yaeyama Islands, Hateruma Island near from the Ryukyu Trench and the Yonaguni Island near from Taiwan. The dominant trend of fault strikes in the islands of the Ryukyu Arc is NW-SE (Fig. 9).

According to Kubo and Fukuyama (2003), several studies have found both arc-perpendicular and arc-parallel extensions between 0.5 and 12 Ma on most islands (Fabbri and Fournier, 1999; Fabbri, 2000; Fournier et al., 2001). This total paleo-stress field might include both the stress field during the episodic opening period of the OT and that during periods without active opening. On the other hand, it is reported the existence of E-W strike slip regime on the Ryukyu Group (Quaternary formation) in the Yonaguni Island and the Hateruma Island (Otsubo and Hayashi, 2003).

6. Finite Element Modeling

6.1 Finite Element Method

To calculate distributions of stress, strain and displacements, we use the FE simulation software package developed by Hayashi (2008), which include elastic FE problem and fault analysis. In term of tectonics and structural geology, a lot of FE modeling studies has been performed after 1996 (e.g. Joshi and Hayashi, 2008; Chamlagain and Hayashi, 2008; Hayashi, 2008 and reference therein).

The model used here is a two-dimensional model that includes a variety of subdomains with different material properties, in order to represent mechanical behavior of different regions. In performing the FE simulation, it is assumed here that the geological materials involving in the analysis are homogeneous and perfectly elastic.

6.2 Configuration of model

In order to detect boundary condition at the Ryukyu Trench, model is bounded along the Ryukyu Trench. For example, Hu et al. (1996) constructed 800 km×800 km rectangular model on Taiwan as centre with ten subdomains. Viallon et al. (1986) constructed FE model from Kyusyu to Taiwan collision zone including whole Okinawa Trough to simulate the interaction between collisions and back-arc spreading. The width of the model is around 2000 km. In this study, we constructed 1300 km×600 km model on the Southern Ryukyu Arc referring to Hu et al. (1996), Otsubo and Hayasahi (2003) and Nakamura (2006). FE model is adopted along plate boundary (Fig. 1). This is based on the idea that plate geometry is significant component of geodynamics of plate margin. FE model include 656 points and 1200 elements.

6.3 Rock domain properties

We divided the studied region into three domains, shown in Fig. 11, with three different physical properties of rocks (density, Young's modulus and Poisson's ratio given in Fig. 10). The Ryukyu Arc and southern side of Taiwan is regarded as the arc region, we set up density is 2600 kg/m3, Young's modulus is 30 GPa and Poisson's ratio is 0.25. The Okinawa Trough is regarded as weak zone and we set up density is 2500 kg/m3, Young's modulus is 5 GPa and Poisson's ratio is 0.25. Rest part is regarded as stable continental margin of EUR plate, we set up density is 2500 kg/m3, Young's modulus is 60 GPa and Poisson's ratio is 0.25. We decided physical property of rocks referring to Otsubo and Hayashi (2003). Additionally, attempted to investigate the effect of rheological difference we constructed single domain model (Fig. 11), with uniform physical property as same as the arc region, shown in Fig. 10. Depth is varied to 1 km, 10 km and 30 km. It is well known that mass is calculated from density. Gravity is calculated from mass and gravitational
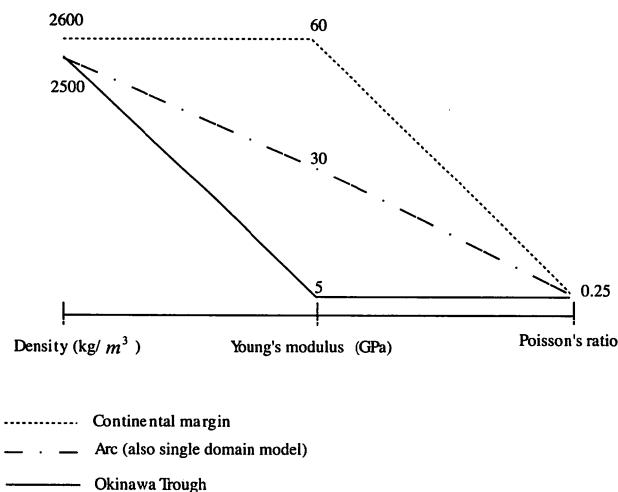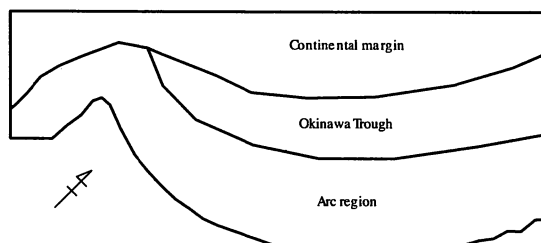
Fig.10. Rock domain properties.

(A) Three domains model
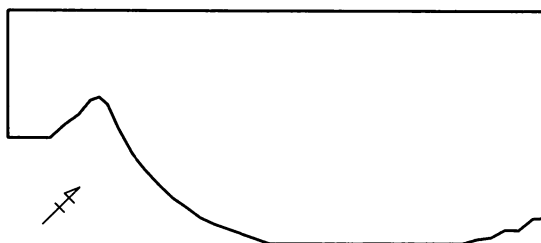

(B) Single domain model

Fig. 11. Model geometry. (A) three domains model and (B) single domain model.

acceleration. Gravity is increase proportionally to the depth.

6.4 Boundary condition

Since the Ryukyu Trench and Taiwan situated on convergence active boundary we consider northeastern, northwestern and southwestern boundaries are rather stable. NW boundary is fixed. SW of Taiwan and NE Ryukyu boundaries can move in NW direction. Half of SW of Taiwan is free to move. We have used four boundary conditions (BC) and are given in Fig. 12. Displacements are given 2000 m that correspond to ca.
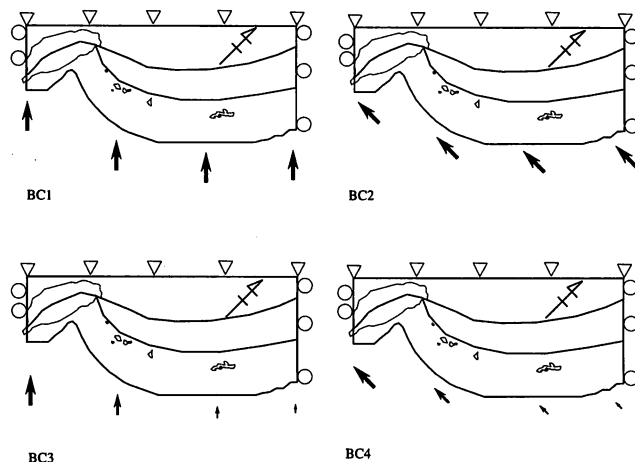
Fig.12. Boundary condition BC1 to BC4. BC1: uniform N45°W displacements on Ryukyu Trench and Taiwan. BC2: uniform EW displacements on Ryukyu Trench and Taiwan. BC3: N45°W displacements on Taiwan gradually decreasing to the north. BC4: EW displacements on Taiwan gradually decreasing to the north.

20,000 years. BC1 is uniform N45°W displacements on the Ryukyu Trench and Taiwan. BC2 is uniform EW displacements on the Ryukyu Trench and Taiwan. BC3 is N45°W displacements on Taiwan and gradually decrease to the north. BC4 is EW displacements on Taiwan and gradually decrease to the north.

7. Results

Three domains model under three variable depths and single domain model under 10 km depth are applied to four boundary conditions, total 16 situations have been simulated. The combinations of experiments are given in Table 1. Results of σ Hmin distribution are visualized to discuss with the T-axis distribution in Figs. 13 to 15. Distribution of displacement vector is given in Figs. 16 and 17.

7.1 Orientation of σ Hmin
7.1.1. Three domains under 10 km depth
Using three domains under 10 km depth, at first we used the boundary condition BC1 that is given in Fig. 12. Result of simulation is showing in Fig. 13. Orientation of σ Hmin is trending NE-SW arc-parallel. Calculated orientations of σ Hmin differ a little from those of the arc, the Trough and continental margin. The difference ascribe to the effect of rock domain properties. Large stress mainly concentrated eastern part of Taiwan. Computed orientation of σ Hmin is good agreement with that of fault slip analysis (Fig. 9) and T-axis distributions (Fig. 8).

In the Okinawa Trough, computed orientation of σ Hmin is arc-parallel. This is inconsistent with observed orientation of σ Hmin (Fig. 8). In Taiwan, orientation of σ Hmin is NE-SW, which is perpendicular to the collision direction. Since this part is collided with PHS plate in the direction of NW-SE, orientation of σ Hmin must be NE-SW. Therefore, orientation of σ Hmin in Taiwan is also good agreement with modeling result (Fig. 8). Hence, orientations of σ Hmin are good agreement with actual stress data.

Next, we have set the boundary condition BC2 to detect the effect of variation in the direction of convergence (Fig. 12). As we know, PHS plate is subducting in the direction of N55°W (Seno et al., 1993) to

the EUR plate. Therefore, we setup the displacement to the EW direction. As a consequence, result shows that σ Hmin is trending NNE-SSW given in Fig. 13. That indicates the direction of subducting PHS plate affects the stress orientation in the arc.

We have also set boundary condition BC3 to detect the effect of variation in the interplate coupling (Fig.12). Interplate coupling is of interest issue in subduction zones. In Taiwan, coupling is considered to be strong, while the southern Ryukyu Arc is considered to be weak decoupling zone. Though Hu et al. (1996) have setup very low rock domain property in the Ryukyu Arc as a weak decoupling zone, in our model we could test directly the effect of variation in the plate coupling. We setup the displacement on the Taiwan part and decrease the volume to the north and zero at northern part. Result shows σ Hmin trends almost same as
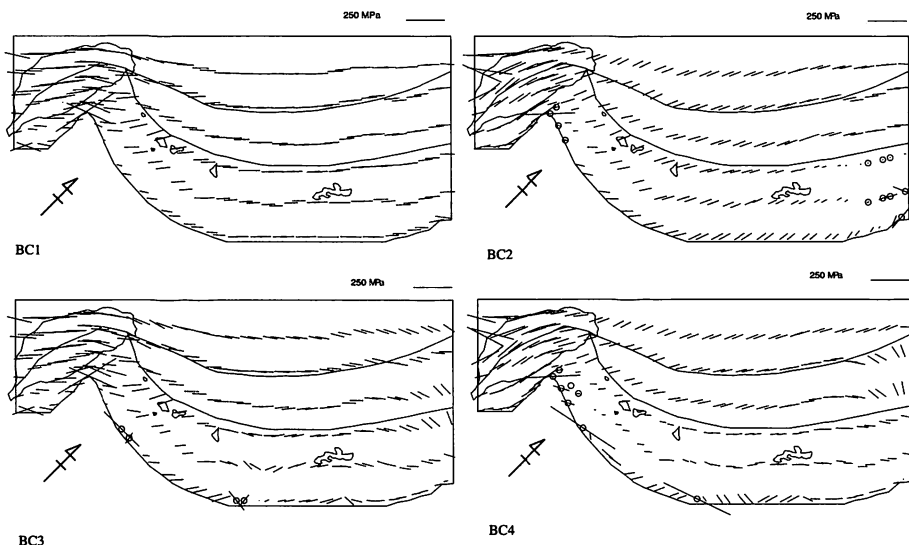

Fig.13. Orientations of σ Hmin of three domains model with boundary condition BC1 to BC4 at 10 km depth.

the result from the boundary condition BC1 (Fig.13), but arc stress orientation in the northern part changed and large stress occurred on southern Ryukyu forearc region. Boundary condition BC4 is a mix of boundary condition BC2 and BC3 (Fig.12). Result is given in Fig. 13 and shows non-uniform σ Hmin distributions through the arc.

7.1.2. Single domain under 10 km depth

Single domain model is constructed to detect the effect of rock domain properties (Fig. 11). Calculated distributions of σ Hmin under boundary condition BC1 under 10 km depth are shown in Fig. 14. The orientations of σ Hmin are almost same but relatively uniform than the results of three domains model.

7.1.3. Three domains under 1 km depth

To discuss the relationship between the geological observation and FE simulation, σ Hmin under 1 km depth is calculated. Result shows orientations of σ Hmin is almost same as under 10 km depth (Fig. 15). However, the magnitude of σ Hmin is quite smaller than that of 10 km depth and larger volume of stress has developed in southern Ryukyu forearc.

7.1.4. Three domains under 30 km depth

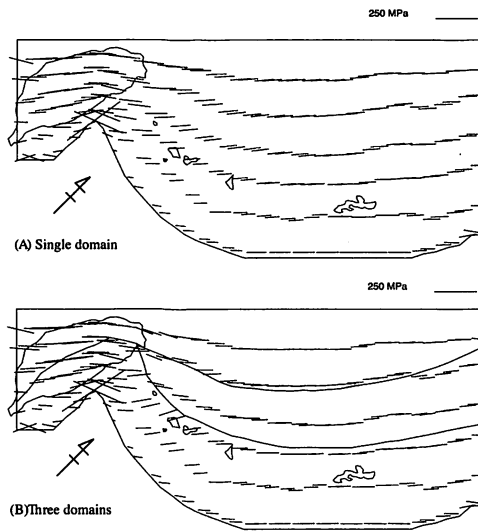Finally, σ Hmin under 30 km depth are calculated to evaluate relationship between focal mechanism

Fig.14. Orientations of σ Hmin of (A) single domain and (B) three domains model with boundary condition BC1 at 10 km depth.
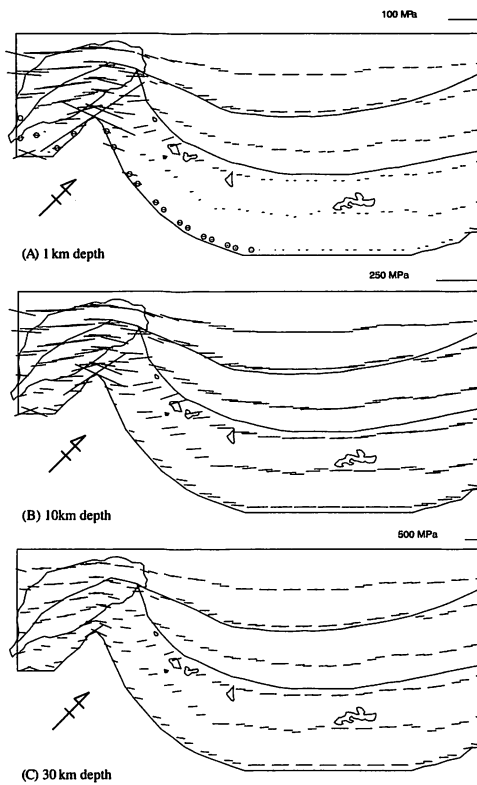

Fig.15. Orientations of σ Hmin of three domains model with boundary condition BC1 at (A) 1 km, (B) 10 km and (C) 30 km depth.
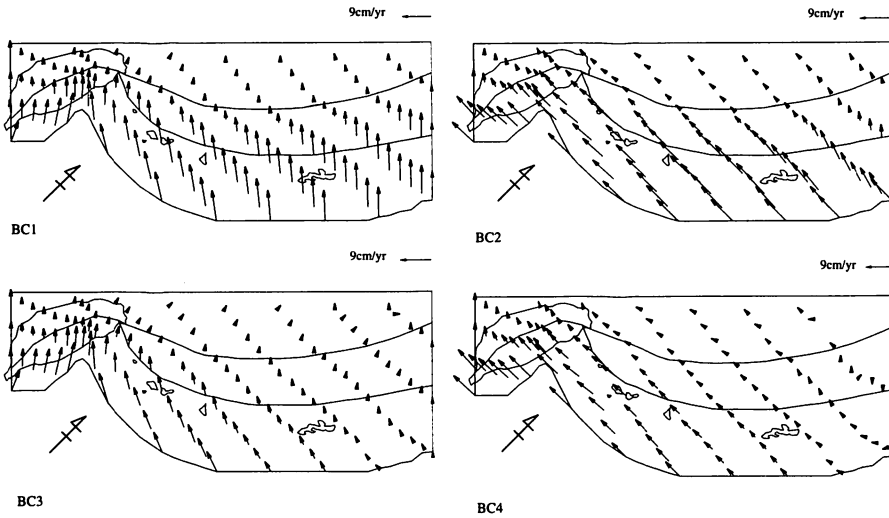
Fig.16. Displacement vector of three domains model with boundary condition BC1 to BC4 at 10 km depth.

solutions of shallow depth earthquake (Fig. 8). Result shows that orientations of σ Hmin is almost same as under 10 km depth (Fig. 15). But magnitude of σ Hmin is larger than that under boundary condition BC1 at 10 km depth.

7.2. Displacement vector distributions

7.2.1. Three domains under 10 km depth

Using three domains under 10 km depth, simulation has performed in boundary condition BC1 to BC4. Displacement vectors are shown in Figs. 16. The dominant directions of displacement vectors are trending northwest in BC1 and BC2, trending west in BC2 and BC4. In general, displacement is small on the continental margin. In the Ryukyu Arc, directions of displacement vectors are trending NW or W, indicating
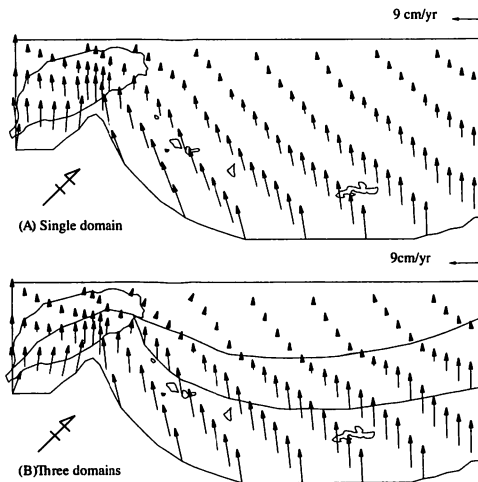

Fig.17. Displacement vector of (A) single domain and (B) three domains with boundary condition BC1 at 10 km depth.

that this model does not fit in this region (Fig.6). However, in Taiwan BC1 and BC3 are rather good agreement with observed velocity field (Fig. 5).

7.2.2. Single domain under 10 km depth

Displacement vector distributions of single domain under 10 km depth are further calculated. Result shows that displacement is more uniform than that under three domains model (Fig. 17).

7.2.3. Three domains under 1 km and 30 km depth

Displacement vectors of three domains under 1 km and 30 km depth are also calculated though they are not shown here. Results are quite similar under 10 km depth model. There is no variation on depth.

8. Discussion

8.1. Misfits

Using oblique subduction of PHS plate model, forearc sliver stress state was simulated. However, this model has two significant problems. First, simulated σ Hmax of Okinawa Trough shows arc-perpendicular direction but the measured σ Hmax of Okinawa Trough shows arc-parallel direction. This fact is supported geological data (Letouzey and Kimura, 1986; Furukawa, 1991; Sibuet et al., 1995; Park et al., 1998), geodetic data (Imanishi et al., 1996; Nishimura et al., 2004) and seismological data (Kubo and Fukuyama, 2003), although GPS sites are limited due to scattered in the Ryukyu Islands. Because the Ryukyu-Kyushu Arc is considered to be seismic decoupling at the Ryukyu Arc (Peterson and Seno, 1984), most researchers consider that the Ryukyu Arc is little deformed by collision of PHS plate. Deformation of the Ryukyu Arc is simulated in this study considering that the Ryukyu Arc is deformed by collision of PHS plate. Seno and Yamanaka (1998) studied the mechanism of back-arc spreading by comparison of over the world subduction zone with back-arc stress and upper slab stress. They reveal significant relationship between the slab stress and the back-arc stress although we do not take into account the slab stress in this study because of limitation in the two-dimension simulation. Recently, seafloor geodetic observations are on going at the Ryukyu Arc from January 2008 (Nakamura, et al., 2008). Their observation will make us possible to know the plate coupling precisely.

Secondary, simulated direction of displacement vector is NW-W trending which is opposite from GPS measurements (Imanishi et al., 1996; Nakamura, 2004; Nishimura et al., 2004; Watabe and Tabei, 2004). It is obvious because of NW-W push displacement as boundary condition. The Ryukyu Arc is moving southward and the northern part of Taiwan, Ilan plain is also moving southward (Hou et al., in press) while Taiwan collision zone is highly deformed and moving north-westward (Hu et al., 2001). This southward motion of the southern Ryukyu Arc is usually not well explained by numerical model (Hu et al., 1996, 2001) because of uncertainty in plate coupling at the Ryukyu Trench. The present model can also not well explain it.

8.2. Model set up and assumption

We set up simplified three subdomains model, although Hu et al. (1996) construct FE model of Taiwan

(A) 3 domains model		
4 BC × 3 depth (1 km, 10 km, 30 km)= 12 experiments		
(B) Single domain model		
4 BC × 1 depth (10 km only)= 4 experiments		

Table.1. Combination of the experiments. Total 16 experiments are performed.

with six subdomains. Because we focus on Southern Ryukyu Arc rather than Taiwan present study simplified these physical differences of Taiwan. We adopted SW boundary on Ryukyu Trench to examine its geometry of Taiwan-Ryukyu junction. We could analyze the effect of plate boundary geometry in this study. Stress magnitude was further increase if the depth is large. This might be because of gravity load and reaction based on Poisson's ratio although this program is two-dimensional.

Which is the best-fit model? We consider boundary condition BC1 is more proper than other boundary conditions. Both single domain and three domains model show rather good agreement with observed stress data. We have performed simulations under 1, 10 and 30 km depth, but we did not find any important difference depending on the depth. As a consequence, we supported that the best model is three domains model with boundary condition BC1 under 10 km depth.

9. Conclusions

FE model has designed to investigate dynamics of the Southern Ryukyu Arc based on synthesized stress-strain, velocity, geology and seismicity data. On the basis of modeling results, we can draw following conclusions:

1. Result of simulation shows that σ Hmin orientations in Taiwan and the Ryukyu Arc are good agreement with T-axis distribution. In addition, relatively large stress has concentrated on the eastern part of Taiwan.
2. In the Okinawa trough, computed σ Hmin orientation is arc-parallel extension. This is inconsistent with actual stress distribution.
3. Result of simulation shows that the direction of calculated displacement vectors is good agreement with observed velocity field in Taiwan.
4. Displacement of single domain model is more uniform than that of three domains model. In addition, displacement vector do not depend on the depth.
5. Directions of displacement vectors are trending NW or W in the Okinawa Trough and the Ryukyu Arc, indicating that this model does not fit in this region.
6. Depth is great influence of the stress magnitude. But there is no significant difference of σ Hmin orientation depending on the depth.
7. Stress distribution is principally controlled by rock domain properties of major structural zones and the direction of convergence of the Philippine Sea plate relative to Eurasia.

References

Chamlagain, D. and Hayashi, D., 2008. FE modeling of contemporary tectonic stress in the India-Eurasia collision zone. Bull.Fac.Sci.Univ. Ryukyus, No.85, 39-79. (http://www.lib.u-ryukyu.ac.jp/)

Fabbri, O., 2000. Extensional deformation in the northern Ryukyu arc indicated by meso-scale fractures in the middle Miocene deposits of Tanegashima Island, Japan. Jour. Geol. Soc. Japan, 106, 3, 234-243.

Fabbri, O. and Fournier, M., 1999, Extension in the southern Ryukyu arc (Japan): Link with oblique subduction and back arc rifting. Tectonics, 18, 3, 486-497.

Fournier, M., Fabbri, O., Angelier, J. and Cadet, J.-P., 2001. Regional seismicity and on- land deformation in the Ryukyu arc: Implications for the kinematics of opening of the Okinawa Trough, J. Geophys. Res. 106, 13751-13767.

Fujii, Y. and Kizaki, K., 1983. Geology and structure of the Yaeyama metamorphic rocks, Ryukyu Islands.

Mem. Geol. Soc. Japan, 22, 15-26. (in Japanese with English abstract)

Furukawa, M., 1991. Formation age of the Ryukyu arc-Okinawa trough system. Japanese Journal of geography, 100, 4, 552-564. (in Japanese with English abstract)

Hayashi, D. and Iguchi, T., 2000, Stress analysis around Ryukyu Arc by means of finite element method. Geoinformatics, 11, 2, 74-75. (in Japanese)

Hayashi, D., 2008. Theoretical basis of FE simulation software package. Bull.Fac.Sci. Univ. Ryukyus, No.83, 29-60. (http://www.lib.u-ryukyu.ac.jp/)

Ho, C.-S., 1986. A synthesis of the geologic evolution of Taiwan. Tectonophysics. 125, 1-16.

Hou, C.-S., Hu, J.-C., Ching, K.-E., Chen, Y.-G., Chen, C.-L., Cheng, L.-W., Tang, C.-L., Huang, S.-H. and Lo. C.-H., in press, Tectonophysics.

Hsu. S-K., Sibuet, J-C., Monti, S., Shyu, C-T. and Liu, C-S., 1996. Transition between the Okinawa trough backarc extension and the Taiwan collision: New insights on the southernmost Ryukyu subduction zone. Marine Geophysical Researches, 18, 163-187.

Hu, J.-C., Angelier, J., Lee, J-C., Chu, H-T. and Byrne, D., 1996. Kinematics of conver- gence, deformation and stress distribution in the Taiwan collision area: 2-D finite- element numerical modeling. Tectonophysics, 255, 243-268.

Hu, J.-C., Yu, S.-B., Angelier, J. and Chu, H.-T., 2001. Active deformation of Taiwan from GPS measurements and numerical simulations. J. Geophys. Res., 106, 2265-2280.

Imanishi, M., Kimata, F., Inamori, N., Miyajima, R., Okuda, T., Takai, K., Hirahara, K. and Kato, T., 1996. Horizontal displacements by GPS measurements at the Okinawa?Sakishima Islands (1994-1995). Jishin (J. Seismol. Soc. Jpn), Ser. 2. 49, 417-421. (in Japanese with English abstract)

Iwasaki, T., Hirata, N., Kanazawa, T., Melles, J., Suyehiro, K., Urabe, T., Moller, L., Makris,J. and Shimamura, H., 1990. Crustal and upper mantle structure in the Ryukyu Island Arc deduced from deep seismic sounding. Geophys. J. Int.,102, 631-651.

Joshi, G, R. and Hayashi, D., 2008. FE stress analysis and Quaternary deformation in the fold-and-thrust belt of the Garhwal Himalaya. Bull.Fac.Sci.Univ. Ryukyus.No.85, 1-37. (http://www.lib.u-ryukyu.ac.jp/)

Kizaki, K., 1985. Geology of the Ryukyu Island Arc. Okinawa Times, 278p. (in Japanese)

Kizaki, K., 1986. Geology and tectonics of the Ryukyu Islands, Tectonophysics, 125, 193-207

Kubo, A. and Fukuyama, E., 2003. Stress field along the Ryukyu Arc and the Okinawa Trough inferred from moment tensors of shallow earthquakes, Earth and Plane. Sci. Lett. 210, 305-316.

Kuramoto, S. and Konishi, K., 1989. Ryukyu Arc is a migrating microplate (forearc sliver). Tectonophysics, 163, 75-91.

Lallemand, S., Liu, C.-S., Dominguez, S., Schnurle, P., and Malavieille, J., 1999. Trench-parallel stretching and folding of forearc basins and lateral migration of the accretionary wedge in the southern Ryukyus: A case of strain partition caused by oblique convergence, Tectonics, 18(2), 231-247.

Letouzey, J. and Kimura, M., 1986. The Okinawa Trough: Genesis of a back-arc basin developing along a continental margin, Tectonophysics, 125, 209-230.

Lu, H. and Hayashi. D., 2001. Genesis of Okinawa Trough and thrust development within accretionary prism by means of 2D finite element method. Kouzou- Chishitu (Structural Geology), 45, 47-64.

Miki, M., 1995. Two-phase opening model for the Okinawa Trough inferred from paleo- magnetic study of Ryukyu arc. J. Geophys. Res., 100, 8169-8184.

Nakamura, M., 2004, Crustal deformation in the central and southern Ryukyu Arc estimated from GPS data, Earth Planet. Sci. Let. 217, 389-398.

Nakamura, M., 2006, Modeling of back arc rifting of the Okinawa trough and arc parallel extension strain in

the south Ryukyu arc by finite element method, Abstract Volume of the Annual Meeting of the Seismol. Soc. Jpn, 157-157. (in Japanese)

Nakamura, M., 2007. Stress field in the subducted Philippine Sea slab at the Ryukyu- Taiwan area, Gekkan Chikyu (The Earth Monthly), 29, 5, 323-328. (in Japanese)

Nakamura, M., Tadokoro, K., Ando, M., Okuda, T., Furukawa, M., Matsumoto, T., Watanabe, T. and Bitou, G., 2008. Observation of seafloor crustal deformation in the Ryukyu trench, Japan Geoscience Union Meeting Poster Session, J164-P014.

Nishimura, S., Hashimoto, M. and Ando, M., 2004. A rigid block rotation model for the GPS derived velocity field along the Ryukyu arc. Phys. Earth Planet. Interior, 142, 185-203.

Otsubo, M. and Hayashi, D., 2003. Neotectonics in Southern Ryukyu arc by means of paleostress analysis, Bull.Fac.Sci.Univ.Ryukyus, No76, 1-73. (http://www.lib.u-ryukyu.ac.jp/)

Park, J-O., Tokuyama, H., Shinohara, M., Suyehiro, K. and Taira, A., 1998. Seismic record of tectonic evolution and backarc rifting in the southern Ryukyu island arc system, Tectonophysics, 294, 21-42.

Peterson, E.T. and Seno, T., 1984. Factors affecting seismic moment release rates in subduction zones, J. Geophys. Res. 89, 10233-10248.

Schnurle, P., Liu, C-S., Lallemand, S. and Reed, D. L., 1998. Structural insight into the south Ryukyu margin: effects of the subducting Gagua Ridge, Tectonophysics, 288, 237-250.

Seno, T., Stein, S. and Gripp, A.E., 1993. A model for the motion of the Philippine Sea Plate consistent with Nuvel I and geological data. J. Geophys. Res., 98, 17941-17948.

Seno, T. and Yamanaka, Y., 1998. Arc stresses determined by slabs : Implications for mechanisms of back-arc spreading, Geophys. Res. Lett. 25, 3227-3230.

Sella, G. F., Dixon, T. H. and Mao, A., 2002. REVEL: A model for Recent plate velocities from space geodesy. J. Geophys. Res., 107(B4), 2081, doi:10.1029/2000JB000033.

Sibuet, J.-C., Hsu, S.-K., Shyu, C.T. and Liu, C.S., 1995. Structural and kinematic evolutions of the Okinawa trough backarc basin, in: B. Taylor (Ed.), Backarc Basins: Tectonics and Magmatism, Plenum, New York, 343-378.

Suppe, J., 1981. Mechanics of mountain building and metamorphism in Taiwan. Mem.Geol. Soc. China. 4, 67-89.

Suppe, J., 1984. Kinematics of arc-continent collision, flipping of subduction, and back-arc spreading near Taiwan. Mem. Geol. Soc. China. 6, 21-33.

Tamaki, K. and Honza. E., 1991. Global tectonics and formation of marginal basins: Role of the western Pacific. Episodes, 14, 3, 224-230.

Teramae, N. and Hayashi, D., 2004, Paleostress transition by fault-striation analysis in the northern and central Ryukyu arc, southwest Japan Bull.Fac.Sci. Univ. Ryukyus,No.78, 163-231. (http://www.lib.u-ryukyu.ac.jp/)

Tsai, Y.B., 1986. Seismotectonics of Taiwan. Tectonophysics, 125, 17-37.

Viallon, C., Huchon, P. and Barrier, E., 1986. Opening of the Okinawa basin and collision in Taiwan: a retreating trench model with lateral anchoring. Earth Planet. Sci. Lett. 80,145-155.

Watabe, T. and Tabei, T., 2004. GPS Velocity Field and Seismotectonics of the Ryukyu Arc, Southwest Japan. Jishin (J. Seismol. Soc. Jpn), Ser. 2, 57,1-10. (in Japanese)

Watabe, T. and Tabei, T., 2006. FEM modeling of the mechanism of back-arc spreading at the Okinawa and Mariana Trough. Abstract Volume of the Annual Meeting of the Seismol. Soc. Jpn, 156-156. (in Japanese)